

# Machine Learning in the calibration process of MercuryDPM Discrete Particle Model: The case with Angle of Repose

Quang Hung Nguyen

Head Supervisor: Thomas Weinhart, Daily Supervisor: Anthony Thornton, Additional member: Chen Kuan.  
Multi-Scale Mechanics Group, Faculty of Engineering Technology, University of Twente.

## 1 Introduction



Figure 1: Examples of Granular Materials.[1]

Granular material is a family of material characterized by its large bulk of densely packed particles, ranging from nanometers to centimeters [2], and is able to resist deformation and form heaps, i.e., behave like a solid and withstand strong shear force [3]. Simple examples of granular materials include sand, gravel, clays, seeds, nuts, and all ranges of powders such as coffee powder, cement powder, which is shown in figure 1. Furthermore, many processes and equipments in chemical plants use granular materials, such as catalysis, adsorption, and heat exchangers. Granular materials are projected to make about half of the products and three-quarters of the raw materials used in the chemical industry [4]. Thus, understanding how granular materials behave is of great significance.

The simulation of granular material's bulk mechanical behavior is done using Discrete Particle Model (DPM, or Discrete Element Method - DEM), which generates the movement of individual particles to capture the macro-scale behavior. The DPM is a family of numerical methods for computing the motion of a large number of particles [5], first proposed by Cundall and Strack in the 1970s [6]. Since the properties of granular materials differ wildly, these simulations require an extensive calibration process designed individually for each type of granular material. Some parameters of the granular material model can be measured directly, such as size distribution or density. However, other parameters are effective parameters (i.e., they result from a simplified particle model) and thus cannot be directly measured. These parameters are then calibrated by choosing a few standard calibration setups (rotating drum, heap test, ring shear cell) and simulating these setups in a DPM simulation,

and the missing parameters are determined such that the response of the experimental and simulation setups match.

Recently, coupled with the raise of Machine Learning in other fields, it has also been applied to solve the calibration problem. This has been done using a Neural Network [7, 8, 9], Genetic Algorithm [10], and a recursive Bayesian sequential Monte-Carlo filtering algorithm named GrainLearning [11]. In this Assignment, two Machine Learning algorithms will be discussed: Neural Network and GrainLearning.

These two algorithms set to treat the calibration problem in two different ways, and likewise, solve it in two different ways: While GrainLearning looks to identify the microparameters from the experimental and DEM simulations's bulk parameters (inverse problem), the Neural Network will help generating a database that can map different microparameters combinations to their corresponding bulk parameters, generated by DEM simulations. In other word, NN will learn the built-in relationship between the micro- and macroparameters of the Discrete Particle Model, thus allow a much faster prediction compare to a full DEM simulation. One advantage of GrainLearning compares to other Machine Learning algorithms such as Neural Network is that it is an unsupervised learning algorithm, i.e., it can starts calibrating with a minimal amount of input information. A normal calibration routine, currently implemented in MercuryDPM would only need the measurements data, parameter range, and the importance weight of each measurement (depends on the modeller's knowledge). Meanwhile, the current approach mentioned in [7, 8, 9] would requires modeller to define a different NN model for each material, train it using a set of DEM simulations, and then validate the correct combinations of input-output by experiment. And although this process can be automated, to date the author has not been aware of any study implemented a fully-automated calibration routine using Neural Network.

**todo here: A paragraph describes each section**

## 2 Experimental Method

### 2.1 Discrete Particle Model

Discrete Particle Model simulates particle motion by applying forces and torques which derives from particle-particle interactions and external influences, on the basis of the given contact law. It performs calculations of kinematics that a given particle  $i$  exerts on other particle  $j$ , for each particle in the system, among with the peripheral factors such as gravity and walls. To achieve this results, the particles are assumes to be (1) undeformable - deform therefore implemented as overlap, (2) unbreakable, (3) all internal interactions are due to particle-particle interaction, (4) Each particle pair  $i, j$  has only one contact point  $c_{ij}$  which the forces and torques act on, and (5) all external forces and torques are either body forces and torques or by interacting with a wall [12].

#### 2.1.1 Contact Laws

For each particle  $i$  on the system, Eq. 1 describes the internal and external forces, and Eq. 2 describes the torque acting on it [12]:

$$F_i = \sum_{j=1}^{n_p} F_{ij} + \sum_{k=1}^{n_w} F_{ik}^w + F_i^b \quad (1)$$

$$\tau_i = \sum_{j=1}^{n_p} r_{ij} F_{ij} + \tau_{ij} + \sum_{k=1}^{n_w} r_{ik} F_{ik}^w + \tau_{ik}^w + \tau_i^b \quad (2)$$

With  $F_{ij}$  interparticle forces,  $F_{ik}^w$  the interaction force between each wall and the particle,  $n_p$  = number of particles,  $n_w$  = number of walls,  $F_i^b$  body forces i.e., gravity, and  $r_{ij}$  as the branch vector, which connects the particle position  $r_i$  with the contact point  $c_{ij}$ . The same hold for torques equation, with  $\tau$  as torque.

The contact law used in the simulations is the Linear Spring-Dashpot model, which is implemented in MercuryDPM as `LinearViscoelasticSpecies`. It defines the interaction between two particles  $i$  and  $j$  as a damped harmonic oscillators [13]:

$$F_{ij}^n = \begin{cases} k_n \delta_{ij}^n + \gamma_n v_{ij}^n & \text{if } \delta_{ij}^n > 0, \\ 0 & \text{else,} \end{cases} \quad (3)$$

In this equation,  $k_n > 0$  represents spring stiffness,  $\gamma_n \geq 0$  represents the damping coefficient,  $v_n$  the normal vector, and  $\delta_{ij}^n$  is the overlap between the particles. Two particles interact with each other if and only if they overlap. This contact model is simple, has an analytic solution and less computationally expensive [14], while also suitable for large particles [12].

### 2.1.2 Angle of Repose

Angle of Repose (AoR) is one of the most important bulk parameters to describe the characteristics of Granular Material. Despite having a generic name, definitions of AoR differs vividly, subject to different applications and behaviors [15]. In the context of this Assignment, two different AoR will be discussed: Static and Dynamic Angle of Repose.

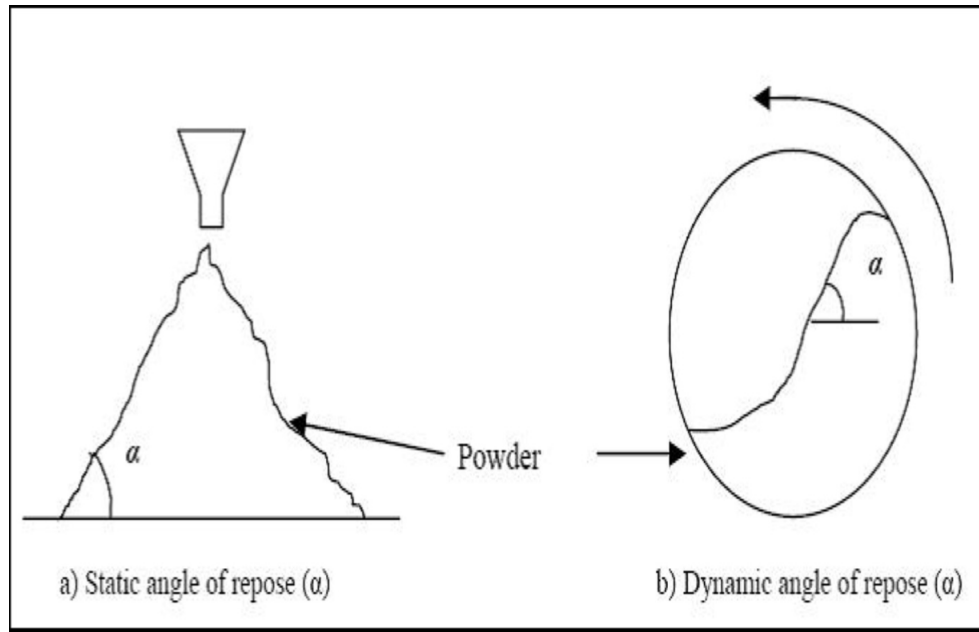


Figure 2: Static and Dynamic Angle of Repose [16].

#### 2.1.2.1 Static Angle of Repose and heap shape measurement

Static AoR, as described in Fig. 2a, is defined as the angle that granular solids forms when it piled with a flat surface, and is essential to characterise the coarseness and smoothness of materials. This in turn can help designing a process involved with the material - lower static AoR implies more flowable and thus easier to transport with less energy [17].

In MercuryDPM, Static AoR is measured by a hollow cylinder simulation. A flat surface is placed at the bottom, and then a cylinder is positioned right on top. After that, the particles are poured into the cylinder, rested, and then the cylinder is removed, which will results in a cone-shaped heap of particles. After the heap is rested, the center of mass of the heap is calculated to determine the height of the cone. The angle results from  $\arctan(\text{height}/\text{diameter})$  is the static AoR. The key point here is to let the heap of particle comes to a fully rested state, i.e., the kinetic energy is negligible compared to the potential energy. This is proved challenging for simulations with low coefficient of friction - which led to an unstable heap.

## 2.2 GrainLearning

GrainLearning is a calibration toolbox developed by Cheng et al., utilizes the recursive Bayesian algorithm to estimate the uncertainty parameters in DPM. Initially, a wide range of parameter space is quasi-randomly sampled from the initial guess range to create a prior distribution of each parameter. Then, conditioned on the experimental values, the posterior distribution of the parameters is updated recursively by Sequential Monte-Carlo Filtering (SMC Filter) and fitted to a Gaussian Mixture Model. This process is done iteratively, until a desired value that minimises the loss function is reach, typically 3 iterations. Algorithm 1 and the following sections will describe in brief the calibration workflow implemented in GrainLearning.

---

### Algorithm 1 GrainLearning

---

**Input:**

**y:** Experimental values  
**x = F(Θ):** DEM solver  
**(Θ<sub>min</sub>, Θ<sub>max</sub>):** Initial guess range

**Main:**

▷ Set uniform prior distribution:  $p(\Theta) = \mathcal{U}(\Theta_{min}, \Theta_{max})$   
**for**  $k$  in range  $(0, K)$  **do**  
    ▷ Sampling parameters:  
    **if**  $k = 0$  **then** sample  $N_p$  parameters values from initial distribution:  $\Theta_k^{(i)} \sim p_0(\Theta)$   
    **else if**  $k > 0$  **then** sample  $N_p$  parameters values from prior distribution:  $\Theta_k^{(i)} \sim p_{k-1}(\Theta \mid y_{1:T})$   
    ▷ Evaluate DPM:  $x_k^{(i)} = F(\Theta_k^{(i)})$   
    ▷ Optimizing  $\sigma$ :  
    **while** True **do**  
        ▷ Compute likelihood (Eq. 4):  $p(y_t \mid \Theta_k^{(i)}) \propto \mathcal{N}(y_{kt} \mid x_{kt}^{(i)}, \Sigma)$   
        ▷ Compute posterior distribution of  $\Theta_k^{(i)}$  conditioned to  $y$  (Eq. 5).  
        ▷ Compute Effective Sample Size (ESS) with Eq. 6.  
        ▷ Stop if target ESS value is reached:  
        **if**  $k = 0$  and  $ESS > 20\%$  **then** break  
        **else if**  $k > 0$  and  $ESS \sim ESS_{max}$  **then** break  
    ▷ Fit sampled posterior distribution to Gaussian Mixture Model:  $p(\Theta \mid y) = \sum_{\alpha}^k \lambda_{\alpha} \mathcal{N}(\mu_{\alpha}, \sigma_{\alpha})$   
    ▷ Set new prior distribution:  $p(\Theta) \leftarrow p(\Theta \mid y)$   
**Output:**  $\Theta_{opt}$  in  $\Theta_K$  that minimizes  $|F(\Theta_{opt} - y)|$

---

### 2.2.1 Posterior distribution calculation

Initially, the measurement is assumed to have an error represented by a covariance matrix  $\Sigma_{\alpha} = \sigma \omega_{\alpha} y_{\alpha}$ , with  $\sigma$  the covariance parameter, and important weight of the measurement  $\omega$ . With  $\Sigma$ , the likelihood of a given state  $\Theta_k^{(i)}$ , i.e., the probabilistic prediction to the experimental data  $y$  can be estimated by the multivariate normal distribution, with  $y_t$  measurement data at time step  $t$ , and  $d$  the dimension of the state vector  $\Theta_k^{(i)}$ :

$$p(y_t \mid \Theta_k^{(i)}) \propto \frac{1}{(2\pi)^{d/2} |\Sigma|} \exp \left( -\frac{1}{2} (y_{kt} - x_{kt}^{(i)})^T \Sigma^{-1} (y_{kt} - x_{kt}^{(i)}) \right) \quad (4)$$

With the calibration system being modelled as a hidden Markov model, the posterior distribution of  $\Theta_k^{(i)}$  can be calculated using recursive Bayes' rule:

$$p(\Theta_k^{(i)} \mid y) \propto \prod_{t=1}^{N_t} p(y_t \mid \Theta_k^{(i)}) p(\Theta_k^{(i)}) \quad (5)$$

### 2.2.2 Effective multi-level sampling

The Effective Sample Size (ESS) is calculated by summing the posterior distribution squared of all the sampled parameters value  $N_p$ :

$$ESS = \frac{1}{N_p \sum_{i=1}^{N_p} p(\Theta_k^{(i)} | y)^2} \quad (6)$$

The main idea is to draw the sample from the previously acquired knowledge about the relationship between  $\Theta$  and  $y$ . In the first iteration ( $k = 0$ ), The uniform prior distribution is chosen as the proposal density, and the parameter spaces are drawn from there. Subsequently, for  $k > 0$ , the proposal density will be the posterior distribution from the previous iteration  $p(\Theta | y)$ . After each iterations, the sampling space will get narrower - therefore, to ensure a proper proposal density for the sampling of parameters, the optimization process will be continued until appropriate  $\sigma$  which maximizes ESS is reached.

## 2.3 Neural Network

Artificial Neural Network (ANN) is a set of algorithms that seeks to identify correlations in data utilizing a technique that inspired by the way human brain operates - mimicking how each neurons in the brain signaling each other. The most basic ANN models is the Feed-forward Multilayer Perceptron Neural Network (MLPNN), in which the purpose is to define the mapping between the input and output  $y = f(x; \theta)$ , and approximate the parameter  $\theta$  which results in the best possible function. In MLPNN, the data will flows in one direction from the input to output, hence the name feed-forward. Like other supervised learning algorithms, a MLPNN need to be trained before it accurately describe the relations between the input and output. This is typically done by feeding the network with pre-labeled data, compare the model's output with the desired output, and update the weights parameter  $\theta$  - a process called backpropagation. In the context of this Assignment, Neural Network (NN) will be used when referring to Feedforward Multilayer Perceptron Neural Network.

### 2.3.1 Designing a Neural Network

In order to choose a correct NN model that can describes the relationship of micro- and macroparameters as indicated in the contact law, a "bottom-up" method is employed.

Initially, a simple one-input one-output NN will be built, to assess how many layers (and neurons) it would take to learn a quadratic relationship  $y = x^2$ , and inverse relationship  $y = 1/x$ .

In the next step, a slightly more complex problem is analysed: a 4-D input and 4-D output model, with contact laws described in table xxx. Finally, a fully-functional model will be coupled with DEM simulations from MercuryDPM.

Certain recommendations will also be taken into account, (7 and 15? )

## 2.4 Experimental procedure

### 2.4.1 Material properties

The material chosen in this experiment is quartz sand, with experimental data provided by Derakhshani et al. [18]. There is no specific interest regarding the choice of material; quartz sand is chosen due to the availability of data and the similarity of measurements.

Table 1: Particle Size Distribution of quartz sand in the simulation

Particle Diameter ( $\mu\text{m}$ )	Cumulative Distribution (%)
300	6.21
425	24.50
500	50.55
600	100

Among with the particle size distribution (PSD) given in Table 1, the fixed parameters in DEM simulations are density  $\rho = 2653 kg/m^3$ , and collision time  $\Delta_t = 6.8 * 10^{-5}$ . Static AoR of quartz sand measured by Derakhshani et al. is  $33^\circ$ .

#### **2.4.2 Heap simulation**

A heap simulation setup consists of two main part: A flat bottom panel and a cylinder, both represented by class `AxisymmetricIntersectionOfWalls`.

### **3 Experimental Result**

#### **3.1 DEM Simulations**

## References

- [1] A. Fernandes, H. Gomes, E. M. B. Campello, P. Pimenta, A fluid-particle interaction method for the simulation of particle-laden fluid problems, 2017. doi:10.20906/CPS/CILAMCE2017-0139.
- [2] A. B. Yu, F. Bassani, G. L. Liedl, P. Wyder, Powder Processing: Models and Simulations, Encyclopedia of Condensed Matter Physics, Elsevier, Oxford, 2005, pp. 401–414. doi:10.1016/B0-12-369401-9/00556-8.
- [3] E. S. Oran, J. P. Boris, R. A. Meyers, Encyclopedia of Physical Science and Technology (Third Edition), Academic Press, New York, 2002, Ch. Fluid Dynamics, pp. 31–43. doi:10.1016/B0-12-227410-5/00248-9.
- [4] R. M. Nedderman, Statics and Kinematics of Granular Materials, Cambridge University Press, Cambridge, 1992, Ch. Introduction, pp. 1–6. doi:10.1017/CB09780511600043.002.
- [5] X. Weng, Modeling of complex hydraulic fractures in naturally fractured formation, Journal of Unconventional Oil and Gas Resources 9 (2015) 114–135. doi:10.1016/j.juogr.2014.07.001.
- [6] P. A. Cundall, O. D. L. Strack, A discrete numerical model for granular assemblies, Géotechnique 29 (1) (1979) 47–65. doi:10.1680/geot.1979.29.1.47.
- [7] L. Benvenuti, C. Kloss, S. Pirker, Identification of dem simulation parameters by artificial neural networks and bulk experiments, Powder Technology 291 (2016) 456–465. doi:10.1016/j.powtec.2016.01.003.
- [8] P. He, Y. Fan, B. Pan, Y. Zhu, J. Liu, D. Zhu, Calibration and verification of dynamic particle flow parameters by the back-propagation neural network based on the genetic algorithm: Recycled polyurethane powder, Materials 12 (20) (2019). doi:10.3390/ma12203350.
- [9] D. Schiochet Nasato, R. Queiroz Albuquerque, H. Briesen, Predicting the behavior of granules of complex shapes using coarse-grained particles and artificial neural networks, Powder Technology 383 (2021) 328–335. doi:10.1016/j.powtec.2021.01.029.
- [10] H. Q. Do, A. M. Aragón, D. L. Schott, A calibration framework for discrete element model parameters using genetic algorithms, Advanced Powder Technology 29 (6) (2018) 1393–1403. doi:10.1016/j.appt.2018.03.001.
- [11] H. Cheng, T. Shuku, K. Thoeni, H. Yamamoto, Probabilistic calibration of discrete element simulations using the sequential quasi-monte carlo filter, Granular Matter 20 (1) (2018) 11. doi:10.1007/s10035-017-0781-y.
- [12] T. Weinhart, L. Orefice, M. Post, M. P. van Schrojenstein Lantman, I. F. Denissen, D. R. Tunuguntla, J. Tsang, H. Cheng, M. Y. Shaheen, H. Shi, P. Rapino, E. Grannonio, N. Losacco, J. Barbosa, L. Jing, J. E. Alvarez Naranjo, S. Roy, W. K. den Otter, A. R. Thornton, Fast, flexible particle simulations — an introduction to mercurydpm, Computer Physics Communications 249 (2020) 107129. doi:10.1016/j.cpc.2019.107129.
- [13] S. Luding, Cohesive, frictional powders: contact models for tension, Granular Matter 10 (4) (2008) 235. doi:10.1007/s10035-008-0099-x.
- [14] H. A. Navarro, M. P. de Souza Braun, Determination of the normal spring stiffness coefficient in the linear spring-dashpot contact model of discrete element method, Powder Technology 246 (2013) 707–722. doi:10.1016/j.powtec.2013.05.049.
- [15] H. M. Beakawi Al-Hashemi, O. S. Baghabra Al-Amoudi, A review on the angle of repose of granular materials, Powder Technology 330 (2018) 397–417. doi:10.1016/j.powtec.2018.02.003.
- [16] A. Castellanos, J. M. Valverde, A. T. Pérez, A. Ramos, P. K. Watson, Flow regimes in fine cohesive powders, Phys. Rev. Lett. 82 (1999) 1156–1159. doi:10.1103/PhysRevLett.82.1156.

- [17] T. F. Teferra, Chapter 3 - engineering properties of food materials, in: M. Kutz (Ed.), Handbook of Farm, Dairy and Food Machinery Engineering (Third Edition), third edition Edition, Academic Press, 2019, pp. 45–89. doi:[doi.org/10.1016/B978-0-12-814803-7.00003-8](https://doi.org/10.1016/B978-0-12-814803-7.00003-8).
- [18] S. M. Derakhshani, D. L. Schott, G. Lodewijks, Micro–macro properties of quartz sand: Experimental investigation and dem simulation, Powder Technology 269 (2015) 127–138. doi:[10.1016/j.powtec.2014.08.072](https://doi.org/10.1016/j.powtec.2014.08.072).